

Molecular Fluorescent pH-Probes Based on 8-Hydroxyquinoline

Stefan Kappaun,^a Tanja Sović,^a Franz Stelzer,^a Alexander Pogantsch,^b Egbert Zojer,^{*b,c}
Christian Slugovc^{*a}

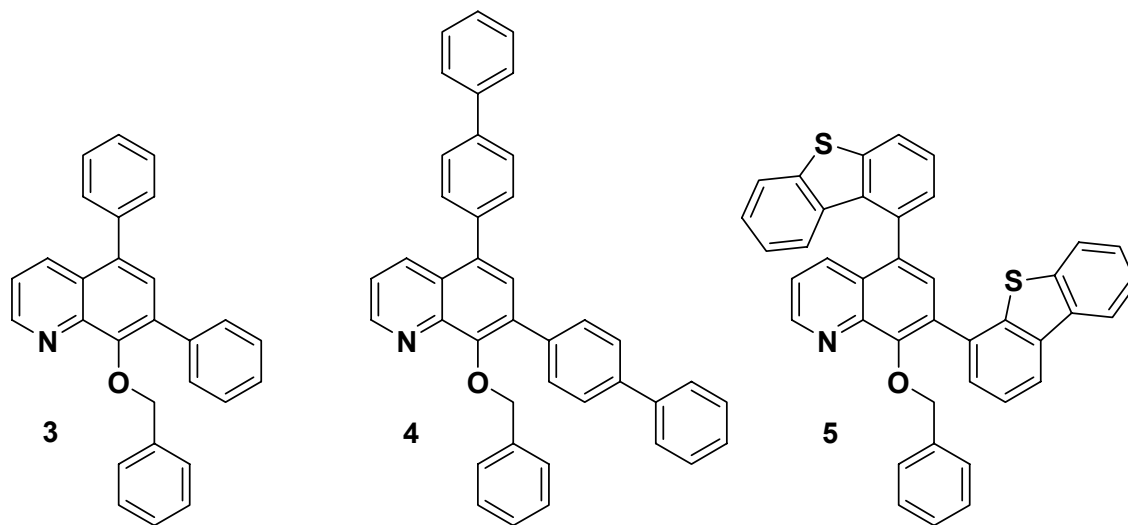
^a Institute of Chemistry and Technology of Organic Materials (ICTOS), Graz University of
Technology, Stremayrgasse 16, A-8010 Graz, Austria

^b Institute of Solid State Physics, Graz University of Technology, Petersgasse 16, A-8010
Graz, Austria

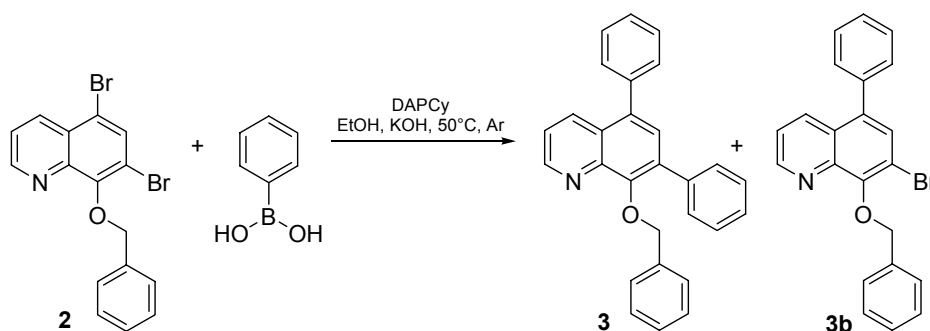
^c School of Chemistry and Biochemistry, Georgia Institute of Technology, 770 State Street,
Atlanta, GA 30332-0400, USA

Electronic Supporting Material

Compounds under investigation



Procedure for the Suzuki cross-coupling using [Pd(OAc)₂(NHCy₂)₂] (“DAPCy”):

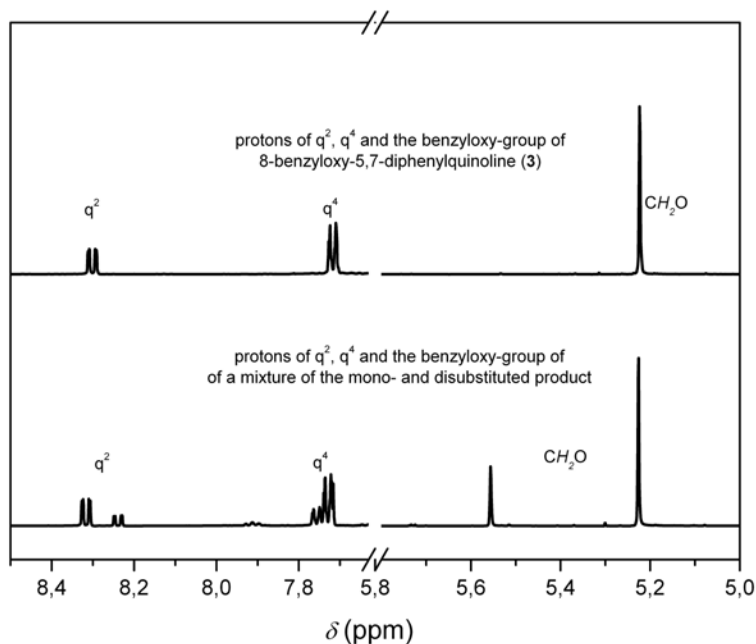


2 (50.0 mg; 0.127 mmol), phenylboronic acid (40.0 mg, 0.328 mmol) and KOH (30.0 mg, 0.535 mmol) were dissolved in degassed EtOH (10 mL) under inert atmosphere of argon and heated to 50°C. After the adding of the catalyst DAPCy (2.0 mg, 0.003 mmol) the reaction mixture was stirred for 12 hours at 50°C. To remove colloidal palladium the reaction mixture was filtered over celite and washed with EtOH and CH_2Cl_2 . Evaporating the solvent gave an orange residue which was tried to purify by column chromatography on silica using cy:ee=5:1. The obtained raw product was identified as a 3 : 1 mixture of **3** and **3b**. It should be noted that we were not able to separate and obtain **3** or **3b** in pure form even using other solvent mixtures for column chromatography.

Attempts to prepare **4** and **5** following this procedure yielded a mixture of mono- and disubstituted products too. Again we were unable to obtain **4** and **5** in pure form using this protocol.

In the following Figure S1, characteristic ¹H-NMR signals for **3** and the mono-phenylated product (**3b**) are shown.

Figure S1 ¹H-NMR signals of characteristic peaks for **3** and **3b**.



General procedure for the measurement of the absorption spectra:

UV-Visible absorption spectra were recorded on Cary 50 Bio UV-Visible Spectrophotometer. Absorption spectra of the solvent mixture were recorded by the measurement of 1000 μL of the pure solvent or 1000 μL solvent + 10 μL TFA conc., respectively (background correction vs. air).

For the measurement of the UV-Visible absorption spectra of **2**, **3**, **4** and **5** background correction using the pure solvent mixture (not acidified!) was performed.

Respectively 1.0 mg of **2**, **3**, **4** and **5** were dissolved in 10 mL of $\text{CHCl}_3/\text{MeOH}$ (1:1). 50 μL from these stock solutions were further diluted with 950 μL of the solvent mixture. For the measurement of the acidified forms 10 μL of a diluted TFA-solution (10 μL TFA conc. + 2000 μL $\text{CHCl}_3/\text{MeOH}$ (1:1)) were added. Further adding of TFA conc. (10 μL) indicated that complete protonation was not achieved by the diluted TFA-solution (see Figure S3). Additional adding of another 10 μL of TFA conc. did not reveal further changes in the absorption spectra.

Figure S2 Absorption spectra of the used solvent $\text{CHCl}_3/\text{MeOH}$ (1:1) and $\text{CHCl}_3/\text{MeOH}$ (1:1) + 10mL CF_3COOH conc.

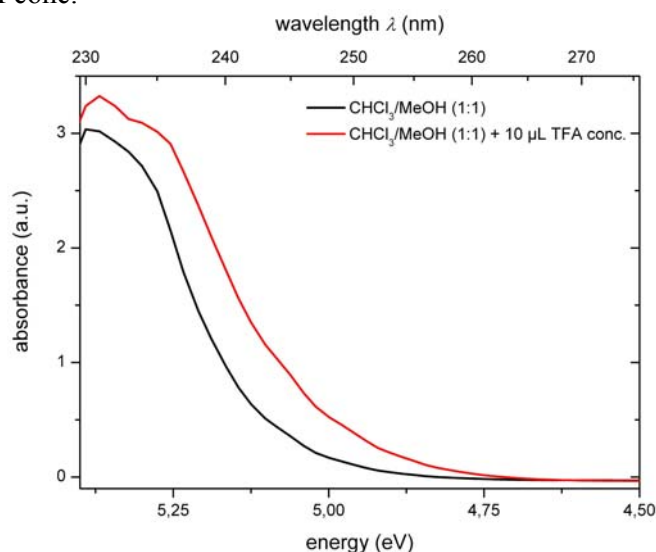


Figure S3 Absorption spectra of **3** in its unprotonated form (black) partly protonated form (green) and presumably fully protonated form (red). On the right calculated absorption spectra (of **3** and **4**) for different protonation ratios are shown. The latter have been obtained by combining the spectra calculated for protonated and non-protonated molecules.

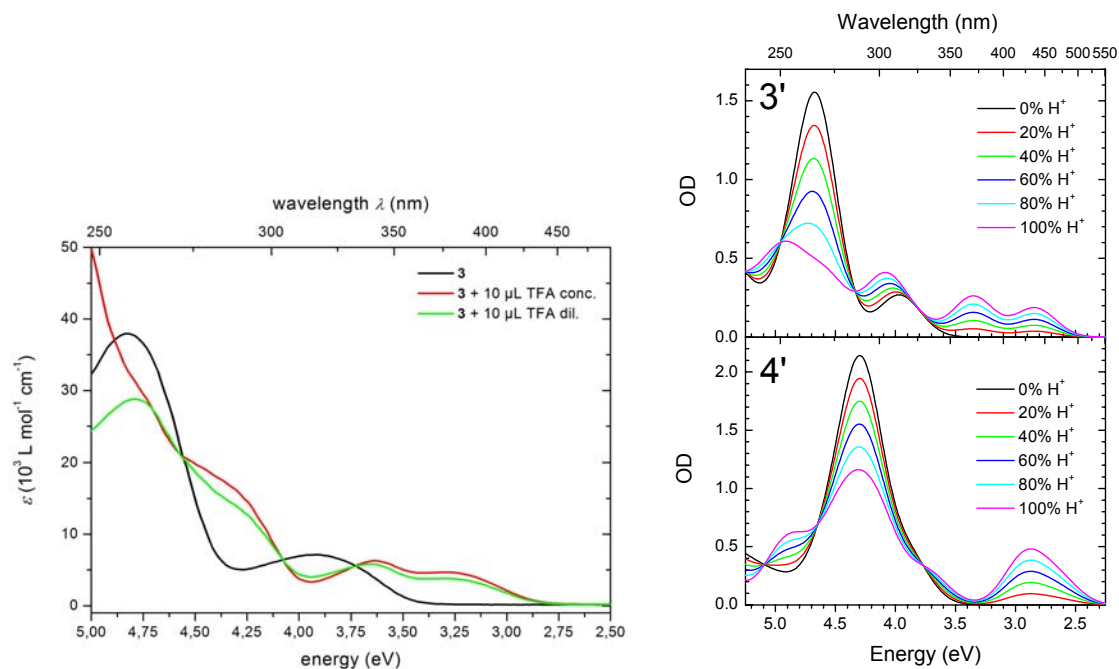


Figure S4 Absorption spectra of **4** (left) and **5** (right) in its unprotonated form (black) and fully protonated form (red).

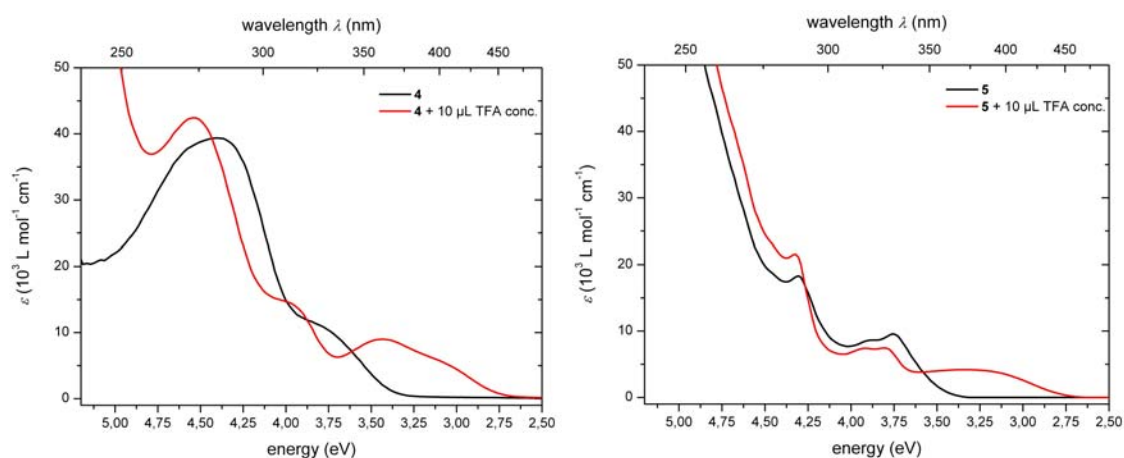


Figure S5 Fluorescence titration of **5** with CF_3COOH ($\lambda_{\text{ex}} = 348 \text{ nm}$).

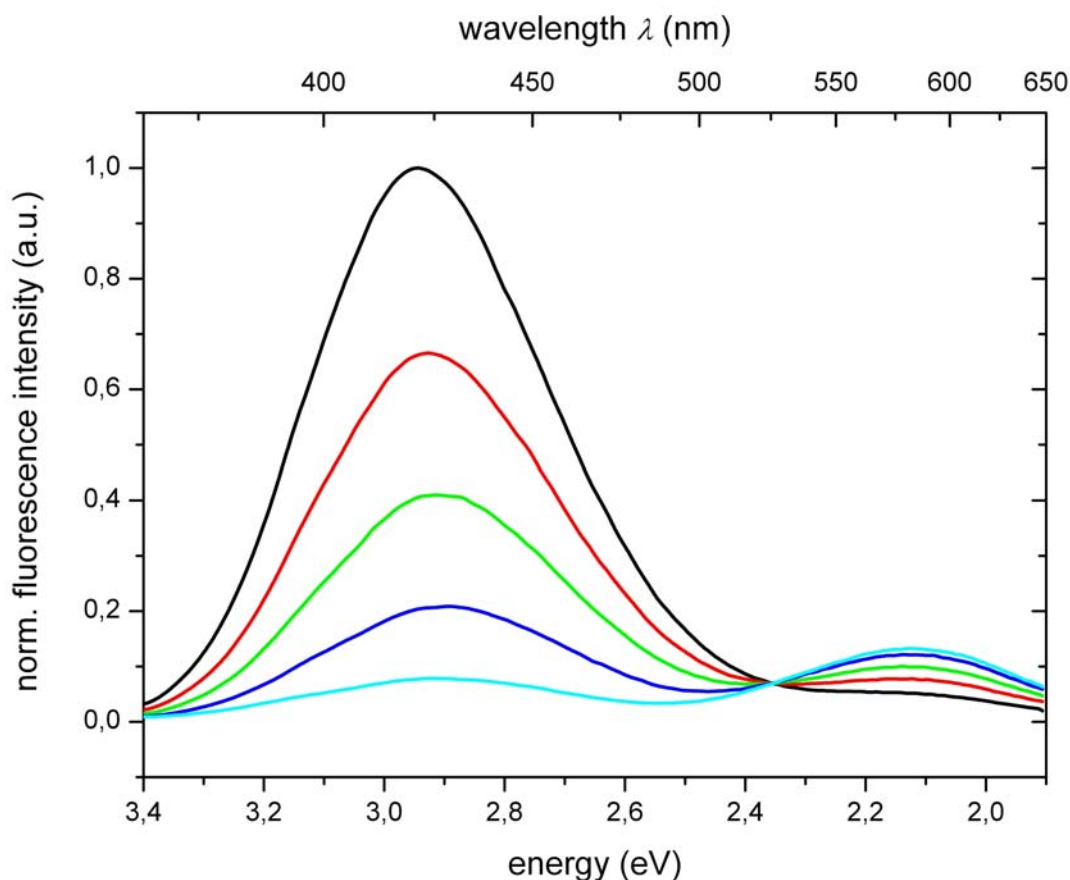


Photo physical properties of **2**, **6**, **7** and **8**

In spite of the fact that it is well known that 8-hydroxyquinoline and its derivatives are almost non fluorescent because of the ESIPT, we investigated the photo physical properties of compounds **1** and **6-8**. The most intense absorption peaks were observed at 251 nm, 269 nm, 277 nm and 241 nm, respectively. The lowest lying absorption maxima were located at 325 nm in case of **1**, 409 nm for **6**, 411 nm for **7** and at 403 nm in the dibenzothienyl substituted derivative **8**. Slight but insignificant changes in the absorption and photoluminescence properties were observed by adding 10 μL of concentrated TFA which suggests that derivatives **6**, **7** and **8** are already partly protonated in the measurements of the alleged non-protonated derivatives which is also supported by the presence of a weak red shifted peak in the corresponding photoluminescence spectra (**6**: 395 and 505nm; **7**: 410 and 525 nm; **8**: 399 and 525 nm - irradiative excitation at 348 nm in all cases). Nevertheless no significant increase of the low energy emission features occurred upon addition of TFA. An exception constitutes **1** which showed the identical absorption spectrum regardless the presence or absence of extra acid. Upon deprotonation of the *OH*-functionality by addition of KOtBu dissolved in $\text{CHCl}_3/\text{MeOH}$ (1:1), the absorption spectra of all compounds were altered. In case of **1**, deprotonation occurred as evidenced by the presence of a red shifted lowest lying absorption maximum (395 nm) and the appearance of a new peak in the photoluminescence

spectrum peaking at 518 nm. In case of **6**, **7** and **8**, the situation was somewhat different. The lowest lying absorption maxima shifted to higher energies namely 338, 347 and 332 nm in case of **6**, **7** and **8**. New emission peaks at longer wavelengths with somewhat higher fluorescence intensities when compared to the neutral forms were detected peaking at 538 nm, 540 nm and 520 nm. Compounds **1** and **6-8** as well as their protonated or deprotonated forms exhibited quantum yields below 1 % rendering these materials unsuitable as fluorescent pH-probes.

Absorption spectra are shown in Figure S6 and S7. Fluorescence spectra are shown in Figures S8 and S9.

Figure S6 Absorption spectra of **1** (left) and **6** (right) in their pristine form (black), upon addition of 100 μ L Et_3N (red) and upon addition of TFA (green).

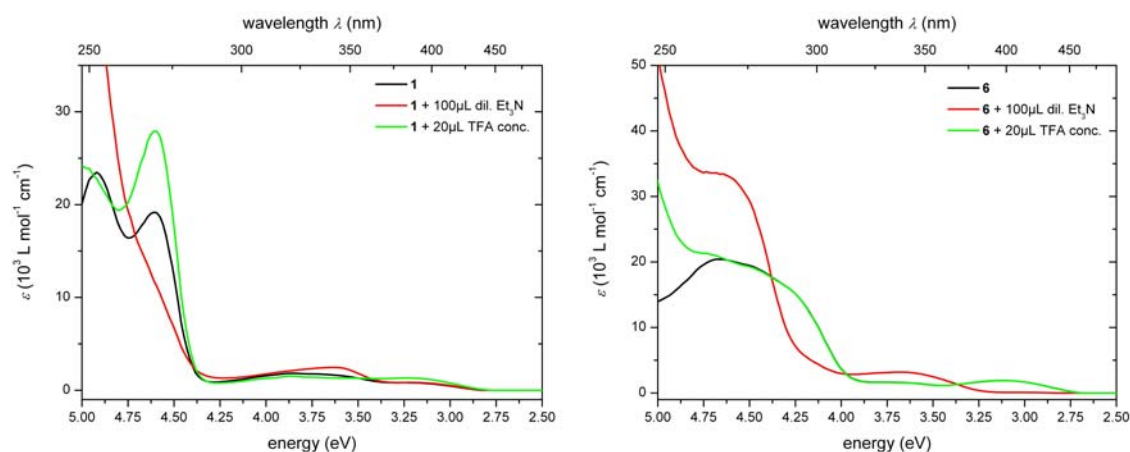


Figure S7 Absorption spectra of **7** (left) and **8** (right) in their pristine form (black), upon addition of 100 μ L Et_3N (red) and upon addition of TFA (green).

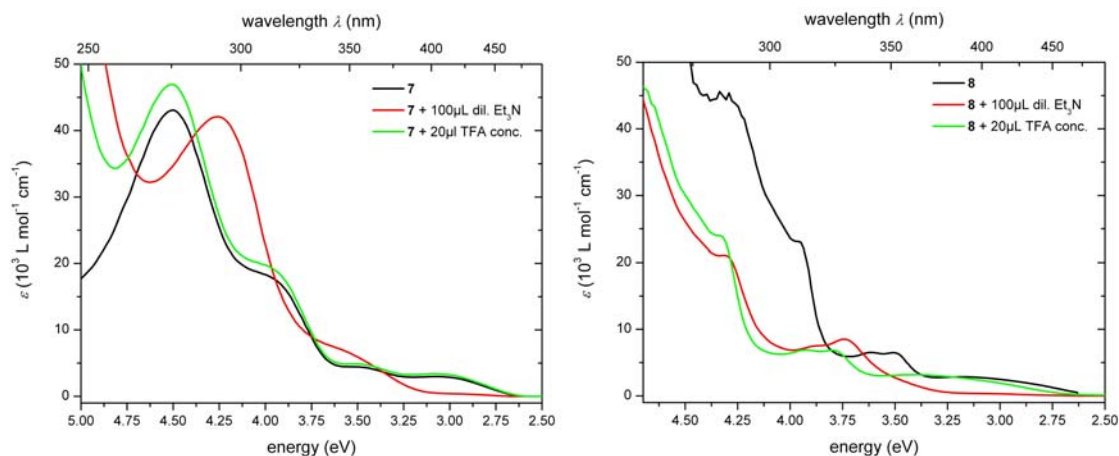


Figure S8 Fluorescence spectra of **1** (left) and **6** (right) in their pristine form (black), upon addition of 100 ml Et₃N (red) and upon addition of TFA (green).

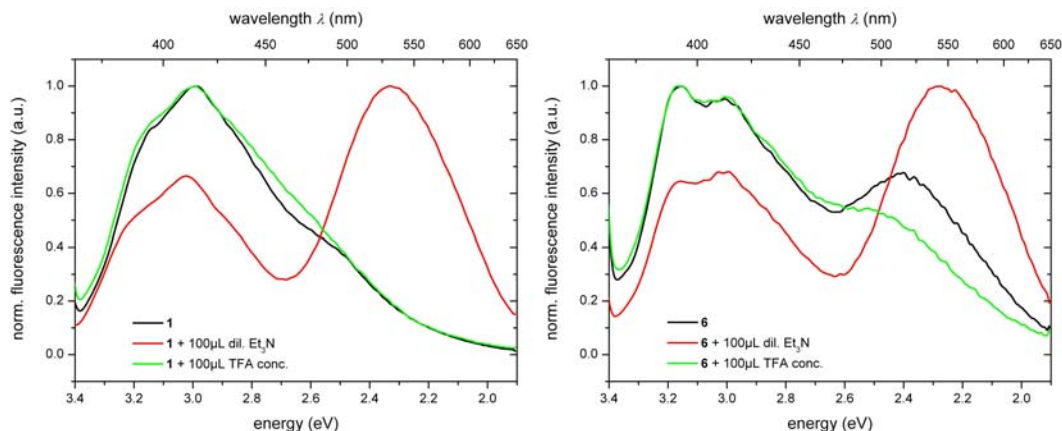
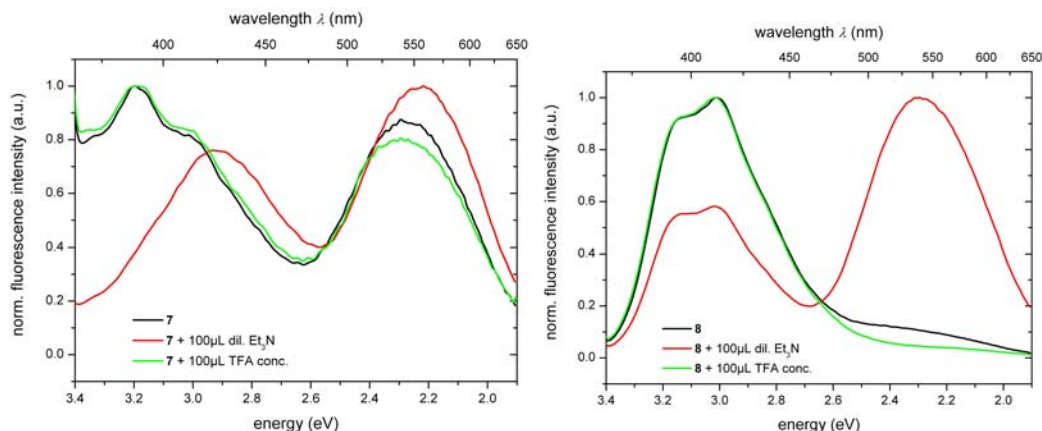


Figure S9 Fluorescence spectra of **7** (left) and **8** (right) in their pristine form (black), upon addition of 100 ml Et₃N (red) and upon addition of TFA (green).



Details regarding the computational methodology

In the INDO-SCI calculations the CI active space has been scaled with the number of π -electrons (i.e., 10 occupied and 10 unoccupied orbitals constitute the CI active space in **2**, 22 occupied and 22 unoccupied in **3** and 34 occupied and 34 unoccupied in **4** and **5**). For the AM1-SCI geometry optimizations various active spaces have been tested including up to 24 (i.e., 12x12) active orbitals. When again scaling the active space with the size of the molecules we fail to simultaneously obtain convergence for all (protonated and non-protonated) molecules for the large active spaces. Therefore, the reported results have been obtained with 2, 4, and 6 active orbitals in molecules **2**, **3**, and **4**. For **5**, the same CI size as in **4** has been chosen. As these small active spaces could induce a bias towards certain excited states in the geometry optimizations, we have performed INDO/SCI calculations on all converged excited state geometries. Only in one case a modified order of the lowest excited states was observed (molecule **3** with a 4x4 active space) and then the optically weak state was only 0.03 eV below the allowed state reported in the paper.

Figure S10 Geometrical conformation of **5'** for which the results in Table S1 and Table 1 in the article have been obtained.

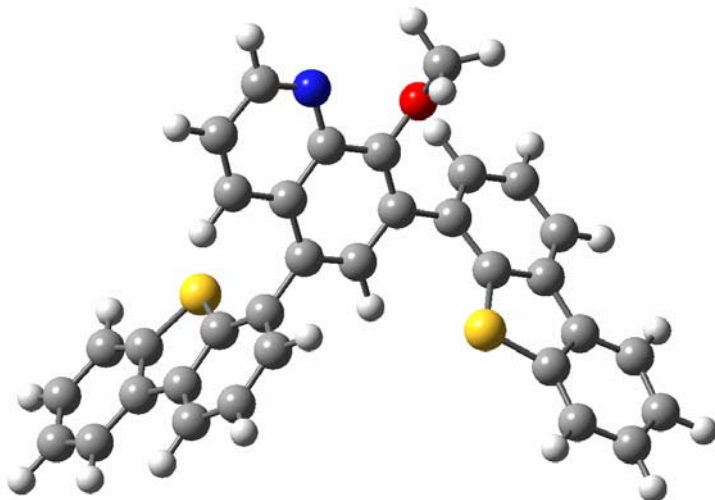


Table S1 INDO/SCI calculated excitation energies, wavelengths, oscillator strengths, and main SCI components of the dominant one-photon states in molecules **2'**, **3'**, **4'**, and **5'**. (H refers to the HOMO and L to the LUMO)

molecule /state	E (eV)	λ (nm)	OS	CI-description
2'				
S ₁	3.96	313	0.00	0.70 (H→L+1) – 0.69 (H-1→L)
S ₄	4.45	279	0.16	0.93 (H→L)
S ₇	5.23	237	0.93	0.58 (H-1→L) + 0.55 (H→L+1) + 0.44 (H-1→L+3)
3'				
S ₁	3.74	332	0.00	0.69 (H→L+1) – 0.52 (H-1→L)
S ₂	3.95	314	0.22	0.88 (H→L)
S ₆	4.65	266	1.37	0.66 (H-1→L) + 0.61 (H→L+1)
S ₇	4.84	256	0.28	0.84 (H→L+2)
4'				
S ₁	3.72	334	0.01	0.51 (H→L+1) – 0.46 (H-3→L)
S ₂	3.89	319	0.38	0.87 (H→L)
S ₄	4.26	291	1.15	0.49 (H→L+1) - 0.50 (H-1→L)
S ₆	4.30	288	0.78	several determinants with similar weights
S ₉	4.56	272	0.53	0.65 (H→L+2) – 0.47 (H-1→L+2)
5'				
S ₁	3.75	331	0.00	0.53 (H→L+3) 0.39 (H-3→L) 0.36 (H-5→L)
S ₂	4.00	310	0.15	0.70 (H→L) 0.44 (H-8→L)
S ₄	4.08	304	0.12	0.58 (H-8→L) 0.52 (H→L)
S ₈	4.49	276	1.43	0.54 (H-1→L+2) 0.39 (H→L+3) 0.38 (H-2→L+1)
S ₉	4.54	273	0.39	0.65 (H-2→L+1) 0.40 (H-1→L+2)
S ₁₀	4.62	268	0.72	0.48 (H→L+2) 0.39 (H-3→L) 0.33 (H-1→L)
S ₁₈	5.33	233	0.50	several determinants with similar weights
				+ several states with OS between 0.2 and 0.5 in the energy range between 5.5 and 5.7 eV

Table S2 INDO/SCI calculated excitation energies, wavelengths, oscillator strengths, and main SCI components of the dominant one-photon states in the protonated species **2'-H⁺**, **3'-H⁺**, **4'-H⁺**, and **5'-H⁺**. (H refers to the HOMO and L to the LUMO)

molecule /state	E (eV)	λ (nm)	OS	CI-description
2'-H⁺				
S ₁	3.42	363	0.11	0.97 (H→L)
S ₄	4.70	264	0.82	0.68 (H→L+1) + 0.59 (H-1→L)
3'-H⁺				
S ₁	2.84	437	0.18	0.79 (H→L) - 0.50 (H-1→L)
S ₂	3.35	370	0.26	0.77 (H-1→L) + 0.45 (H→L)
S ₅	4.08	304	0.30	0.63 (H-4→L) + 0.48 (H→L+1) + 0.40 (H-2→L)
S ₇	4.53	274	0.22	0.75 (H-5→L)
S ₁₁	4.66	266	0.37	0.69 (H→L+2) - 0.60 (H-1→L+2)
S ₁₂	5.06	245	0.22	0.62 (H-1→L+2) + 0.51 (H→L+2)
4'-H⁺				
S ₁	2.64	469	0.21	0.74 (H-1→L) + 0.54 (H-4→L)
S ₂	2.92	424	0.41	0.81 (H→L) - 0.35 (H-1→L)
S ₃	3.74	331	0.26	0.49 (H-4→L+1) + 0.44 (H-1→L+1) + 0.39 (H→L) - 0.32 (H-9→L)
S ₇	4.12	301	0.38	0.66 (H→L+1) - 0.32 (H→L)
S ₈	4.24	293	0.39	0.50 (H-9→L) + 0.45 (H-1→L+1) - 0.34 (H-1→L+2)
S ₁₂	4.44	279	0.49	0.56 (H-1→L+2) + 0.39 (H-1→L+1)
S ₁₉	4.89	254	0.44	0.46 (H-8→L+1) + 0.43 (H-1→L+1)
5'-H⁺				
S ₁	2.88	430	0.24	0.56 (H-4→L) + 0.50 (H-6→L) + 0.41 (H→L) - 0.40 (H-2→L)
S ₅	3.42	363	0.17	0.63 (H-2→L) + 0.59 (H-6→L)
S ₆	3.86	321	0.10	several determinants with similar weights
S ₁₀	4.17	298	0.42	0.48 (H-2→L) + 0.47 (H-4→L) - 0.36 (H-4→L+1)

Figure S11 INDO calculated highest occupied and lowest unoccupied molecular orbitals of **4'** (coloured version of **Figure 3** in the manuscript).

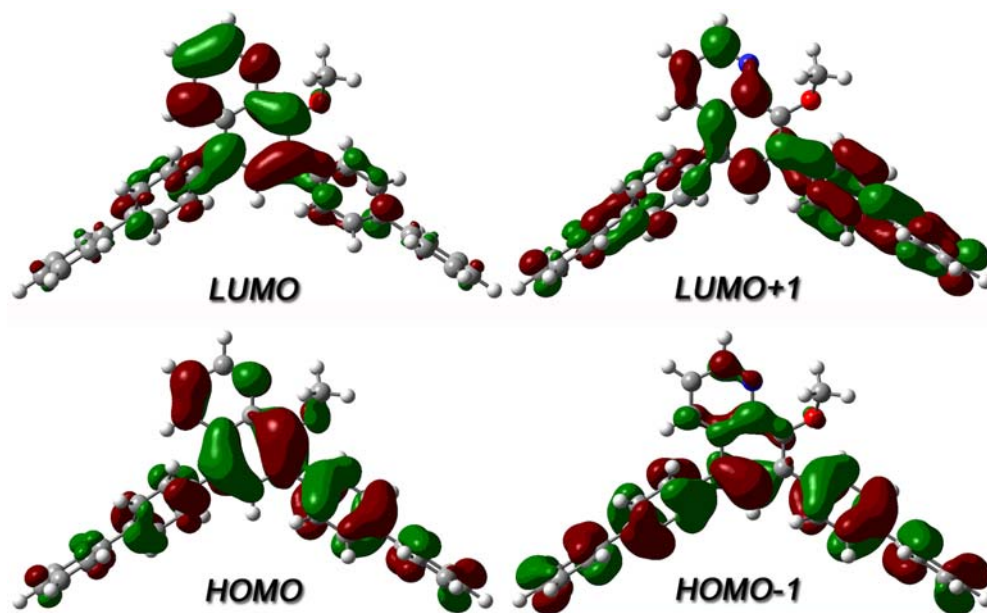
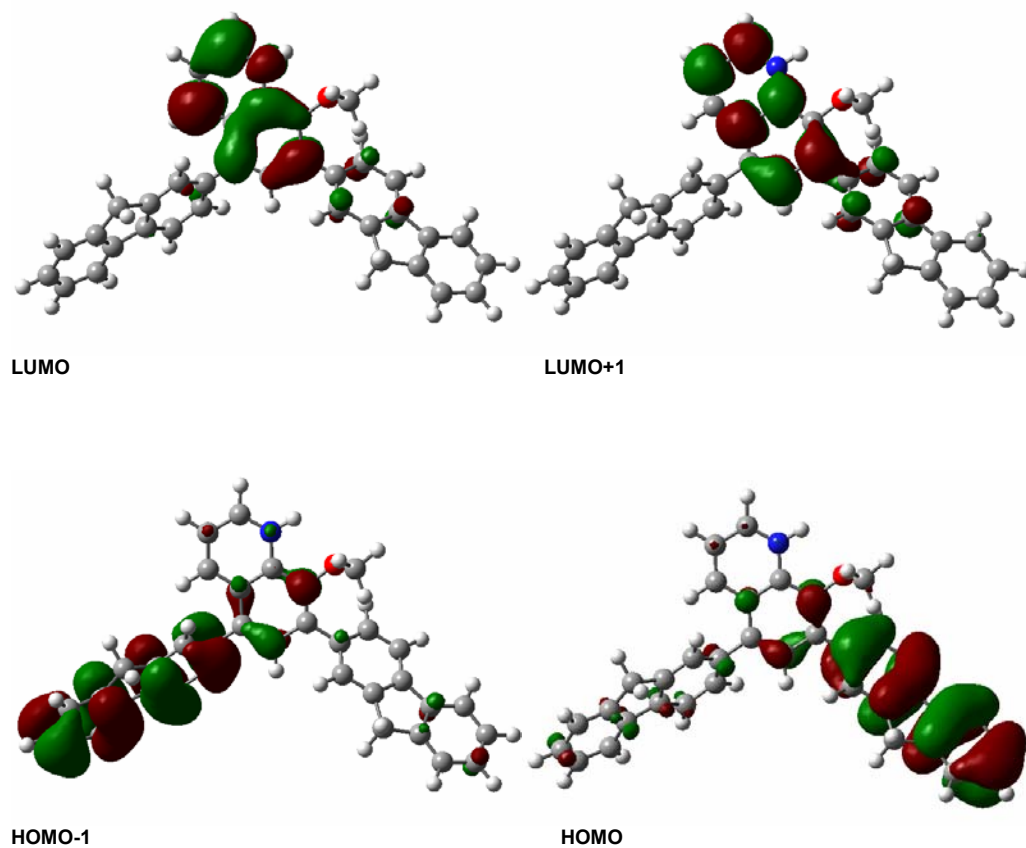
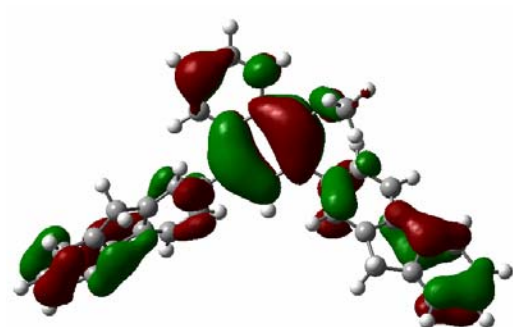


Figure S12 INDO calculated molecular orbitals dominating the CI-descriptions of the two lowest excited states of 4'-H⁺.





HOMO-4

Figure S13 Comparison of the INDO/SCI calculated e-h two-particle wavefunctions for the lowest optically allowed excited states of **4'** (left) and **4'-H⁺** (right) in the ground state (top – compare also Figure 4 of the article) and S_1 state equilibrium geometries (bottom). The shading gives the probability of finding the hole on the site represented by the x-axis, while the electron is on the site given by the y-axis. The numbering of the sites is shown schematically at the top of the figure.

